Acta Mech 229, 497–514 (2018)
https://doi.org/10.1007/s00707-017-1983-4

ORIGINAL PAPER

Jing Yang · Qin Fan · Liangcai Zeng · Leon M. Keer · Kun Zhou

On the plastic zone sizes of cracks interacting with multiple inhomogeneous inclusions in an infinite space

This paper is dedicated to the memory of Franz Ziegler

Received: 19 January 2017 / Revised: 3 April 2017 / Published online: 17 November 2017

Abstract The plastic zones of crack tips play a significant role in the fracture behavior of material. This paper proposes a semi-analytic solution for the plastic zones and stress distribution of an infinite space with multiple cracks and inhomogeneous inclusions under remote stress. In this solution, cracks can be treated as a distribution of edge dislocations with unknown densities according to the distributed dislocation technique, while inhomogeneous inclusions can be modeled as homogeneous inclusions with initial eigenstrain plus the unknown equivalent eigenstrain by using the equivalent inclusion method. These unknowns can be obtained by using the conjugate gradient method. The plastic zones ahead of crack tips are one-dimensional slender strips, and their sizes can be determined by canceling the stress intensity factor (SIF) due to the closure stress and that due to the applied load based on the Dugdale model of small-scale yielding. It is found that the plastic zones of crack tips are significantly affected by Young's modulus and the positions of inhomogeneous inclusions.

1 Introduction

Materials usually contain many micro-defects, such as inclusions, voids, and cracks, which could be formed during the manufacturing or utilization process. They have significant influence on the properties and performance of materials. When the materials with micro-defects were subjected to external loading, the stress concentrations caused by the cracks or inclusions could be serious and might eventually result in material damage. In order to investigate the failure property of materials with micro-defects, the plastic zones of crack tips should be taken into consideration to make the results more accurate. However, it is challenging to obtain the plastic zone sizes of crack tips, when the cracks are interacting with many inhomogeneous inclusions.

In the past few years, the analysis of the elastic deformation of materials with micro-defects has been reported in many works [1–11]. For example, Zhou et al. [12] proposed a semi-analytical solution to study the elastic deformation of an isotropic infinite space with multiple inclusions and cracks by using the equivalent inclusion method (EIM) and distributed dislocation technique (DDT). Tao et al. [13] investigated the effect of an edge dislocation on the interaction between a crack and a circular inclusion under the remote load. However,

J. Yang · K. Zhou (✉)
School of Mechanical and Aerospace Engineering, Nanyang Technological University, 50 Nanyang Avenue, Singapore 639798, Singapore
E-mail: kzhou@ntu.edu.sg

Q. Fan · L. Zeng
The Key Laboratory of Metallurgical Equipment and Control of Ministry of Education, Wuhan University of Science and Technology, Wuhan, China

L. M. Keer
Department of Mechanical Engineering, Northwestern University, Chicago, IL, USA

in all the above studies, only the elastic properties of cracks were considered, which is far from the analysis of actual failure of ductile materials.

In that case, the plastic zones at crack tips play a significant role in determining the crack initiation and propagation [14–18]. The two earliest theoretical works used to estimate the plastic zone sizes ahead of crack tips were performed by Irwin [19] and Dugdale [20]. Generally, the Irwin model was used to estimate the plastic extent ahead of a crack tip. The Dugdale model treated the plastic zones as thin strips ahead of crack tips, and their zone sizes could be determined by canceling the stress intensity factor (SIF) caused by the closure stress and that due to the applied load.

Recently, a few works performed by Xiao's group [21–32] were focused on the plastic zone sizes of a crack interacting with an inclusion. Jing et al. [33] developed an analytical solution for the plastic zones of a semi-infinite crack in an isotropic elastic–plastic solid, based on the von Mises yield criterion and Tresca yield criterion. However, all were obtained with only one crack and one inclusion taken into consideration. Moreover, the interactions between many microcracks and the failure behavior of materials were investigated by Feng et al. [34]. They used a simple and effective method to determine the SIFs of microcracks and provided a potential tool for elucidating some phenomena of material failure, but the effect of plastic zones of the cracks was not taken into consideration. Therefore, the plastic zone sizes of multiple cracks interacting with inhomogeneous inclusions in an infinite space are not available in the previous studies.

The present study aims to propose a semi-analytical solution for the plastic zones and stress distribution in an isotropic infinite space with cracks interacting with multiple inhomogeneous inclusions subjected to a remote load. This solution can take the interaction between inhomogeneous inclusions and cracks into consideration. Based on the Dugdale model, the plastic zone size can be obtained by causing the SIF due to the closure stress and that due to the external loading to vanish [35]. This model can analyze the effect of inclusion parameters on the plastic zone size of crack tips, which provide a guideline for the properties of materials with micro-defects.

2 Methodology

2.1 Problem description and solution approach

In this study, a two-dimensional (xOy Cartesian coordinate system) problem with multiple cracks $\Gamma_\varphi(\varphi = 1, 2, \ldots n)$ and inhomogeneous inclusions $\Omega_\psi(\psi = 1, 2, \ldots m)$ with elastic moduli $C^{\psi}_{ijkl}(i, j, k, l = 1, 2)$ in an isotropic infinite space with C_{ijkl} under external loading σ^{∞}_{yy} is considered, as shown in Fig. 1a. The red lines ahead of cracks represent the plastic zones. Each inhomogeneous inclusion contains initial eigenstrain denoted by ε^{p}_{ij}.

In order to formulate the governing equations to solve the inhomogeneous infinite space problem, cracks can be treated as a distribution of climb and glide edge dislocations with unknown densities $\rho^{\vdash}$ and $\rho^{\perp}$ based on the DDT, while inhomogeneous inclusions can be simulated as homogeneous inclusions with initial eigenstrains ε^{p}_{ij} plus unknown equivalent eigenstrains ε^{*}_{ij} by means of the EIM. Then, this inhomogeneous infinite space problem is transformed into a homogeneous problem as shown in Fig. 1b.

A discretization method is used to solve the governing equations of the proposed problem. The computational domain D, which contains all the cracks $\Gamma_\varphi(\varphi = 1, 2, \ldots n)$ and inclusions $\Omega_\psi(\psi = 1, 2, \ldots m)$ is chosen as shown in Fig. 2. The entire domain is discretized into $N_x \times N_y$ square elements of the same size $2\Delta_x \times 2\Delta_y$. Each element is indexed by a sequence of two integers (α, β) with $0 \le \alpha \le N_x - 1$, $0 \le \beta \le N_y - 1$. The aims of the governing equations are to calculate the unknown equivalent eigenstrains and dislocation densities used to model the inclusions and cracks. Based on the calculation results, the stress distribution in the infinite space can be obtained. Detailed information on the calculation of these unknowns and the stress distribution can be found in the Appendix.

Here, all cracks are assumed as parallel to the x axis. The model is also applicable to vertical cracks without adding extra difficulties. Furthermore, with this method a crack with arbitrary direction can be treated as a zigzag crack consisting of many small vertical and horizontal crack segments.

For sharp cracks, the stresses at crack tips can be theoretically predicted as infinite; however, it is not accurate physically since the radius of the crack tips should be finite in the actual case. By introducing plastic zones ahead of crack tips, the fracture analysis of materials becomes more accurate. Based on the Dugdale model of small-scale yielding, the plastic zones ahead of crack tips are one-dimensional line segments, whose

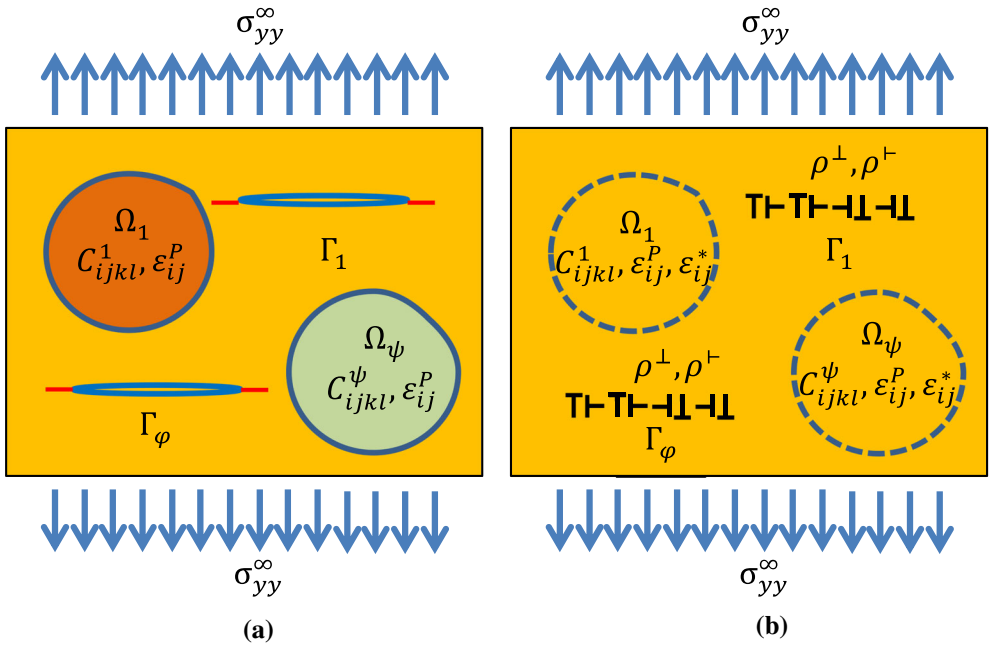

Fig. 1 The original problem of multiple cracks (**a**) and the new problem of multiple dislocation distributions (**b**) under remote stress; the red lines are the plastic zones of crack tips

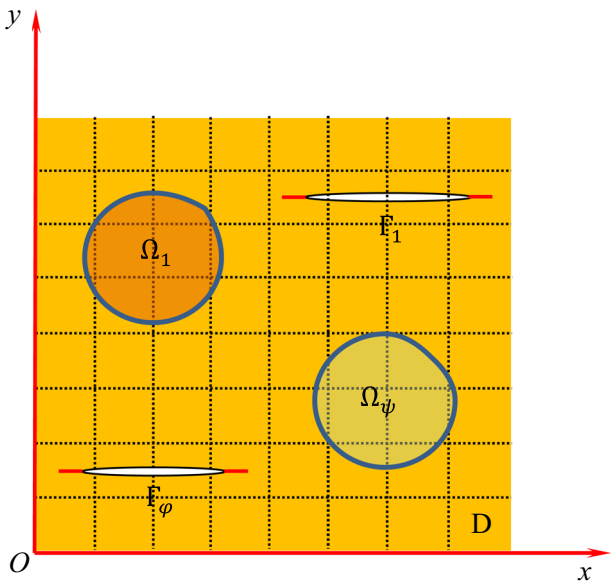

Fig. 2 Discretization of the computational domain with multiple cracks and inclusions into $N_x \times N_y$ elements of the same size

size can be obtained by canceling the SIF due to the closure stress $K_{\mathrm{I}\rho}$ and the SIF due to the applied load K_{I} [35]:

$$K_{\mathrm{I}} + K_{\mathrm{I}\rho} = 0. \tag{1}$$

Due to the presence of inhomogeneous inclusions, the SIFs (K_{I} and K_{II}) exist simultaneously even if only the uniform tensile stress is applied. The condition to obtain the plastic zone size of cracks interacting with inhomogeneous inclusions in an infinite space can be rewritten as follows:

$$\begin{cases} K_{\mathrm{I}}^{\mathrm{L}} + K_{\mathrm{I}\rho}^{\mathrm{L}} = 0 \\ K_{\mathrm{I}}^{\mathrm{R}} + K_{\mathrm{I}\rho}^{\mathrm{R}} = 0 \end{cases}, \quad \begin{cases} K_{\mathrm{II}}^{\mathrm{L}} + K_{\mathrm{II}\rho}^{\mathrm{L}} = 0 \\ K_{\mathrm{II}}^{R} + K_{\mathrm{II}\rho}^{\mathrm{R}} = 0 \end{cases} \tag{2}$$

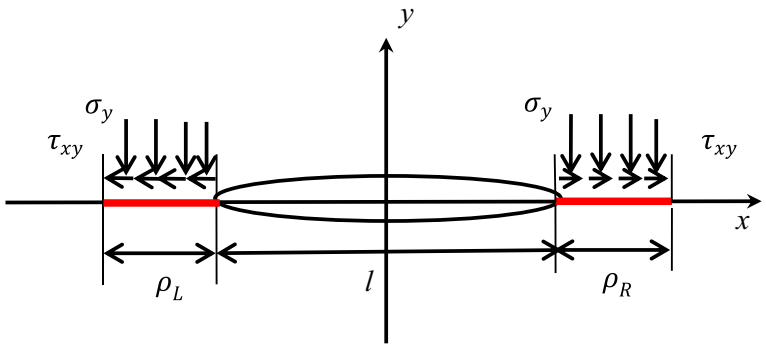

Fig. 3 The plastic zones and yield stress distribution of a Dugdale model crack

where superscripts L and R indicate the left and right crack tips, respectively; the subscripts I and II indicate the Modes I and II crack, respectively.

In order to solve Eq. (2), we need to obtain the relationship between the SIFs ($K_{\mathrm{I}}^{\mathrm{L}}$, $K_{\mathrm{II}}^{\mathrm{L}}$, $K_{\mathrm{I}}^{\mathrm{R}}$, $K_{\mathrm{II}}^{\mathrm{R}}$, $K_{\mathrm{I}\rho}^{\mathrm{L}}$, $K_{\mathrm{II}\rho}^{\mathrm{L}}$, $K_{\mathrm{I}\rho}^{\mathrm{R}}$ and $K_{II\rho}^{R}$) and the plastic zone sizes. The detailed formulas for these SIFs are introduced in Sects. 2.2 and 2.3.

Due to the Dugdale model's assumptions, the length of the plastic zone at the right tip is taken as the same as that at the left tip, and the growth of plastic zones is in the direction of cracks. Thus, the proposed model can be applied in the cases in which the stress distribution around the cracks due to the disturbances of the inhomogeneous inclusions (affected by their locations and material dissimilarities) should satisfy the assumptions.

2.2 Calculation for the SIFs due to the closure stress

Based on the Dugdale model, the effective crack length equals $l + \rho_{\mathrm{R}} + \rho_{\mathrm{L}}$, as shown in Fig. 3. The original crack length is l. The plastic zone size of the right crack tip ρ_{R} should equal that of the left crack tips ρ_{L}, which means that $\rho_{\mathrm{R}} = \rho_{\mathrm{L}} = \rho$. The interactions among the cracks and inhomogeneous inclusions in an infinite space may cause both normal and tangential tractions at the crack tips even though the space is under a simple loading condition, which implies that both Mode I and II SIFs (K_{I} and K_{II}) should be taken into account for the crack tips. Thus, $K_{\mathrm{I}\rho}$ induced by the normal closure stress σ_y and $K_{\mathrm{II}\rho}$caused by the shear closure stress τ_{xy} should be considered, and the stresses at the crack tips should satisfy the von Mises yield criterion. The detailed distribution of the closure stresses $D(x)$ is as follows:

$$
\begin{aligned}
D_y(x) &= \begin{cases} \sigma_y, & \left(-\rho_{\mathrm{L}} - \frac{l}{2} < x < -\frac{l}{2} \text{ and } \frac{l}{2} < x < \frac{l}{2} + \rho_{\mathrm{R}}\right), \\ 0, & (\text{else}) \end{cases} \\
D_x(x) &= \begin{cases} \tau_{xy}, & \left(-\rho_{\mathrm{L}} - \frac{l}{2} < x < -\frac{l}{2} \text{ and } \frac{l}{2} < x < \frac{l}{2} + \rho_{\mathrm{R}}\right), \\ 0, & (\text{else}) \end{cases} \\
&\sqrt{\sigma_y^2 + 3\tau_{xy}^2} = \sigma_{\mathrm{YS}}
\end{aligned}
\tag{3}
$$

where σ_{YS} is the yield stress of the matrix material.

According to fracture mechanics, the SIF due to the normal stress $K_{I\rho}$ and that due to the shear stress $K_{II\rho}$ can be given by

$$
\begin{aligned}
K_{\mathrm{I}\rho} &= -\frac{\sigma_y}{\sqrt{\pi(a+\rho)}} \int_a^{a+\rho} \left\{ \sqrt{\frac{a+\rho+x}{a+\rho-x}} + \sqrt{\frac{a+\rho-x}{a+\rho+x}} \right\} \mathrm{d}x \\
&= -2\sigma_y \sqrt{\frac{a+\rho}{\pi}} \cos^{-1}\left(\frac{a}{a+\rho}\right), \\
K_{\mathrm{II}\rho} &= -\frac{\tau_{xy}}{\sqrt{\pi(a+\rho)}} \int_a^{a+\rho} \left\{ \sqrt{\frac{a+\rho+x}{a+\rho-x}} + \sqrt{\frac{a+\rho-x}{a+\rho+x}} \right\} \mathrm{d}x
\end{aligned}
\tag{4.1}
$$

$$= -2\tau_{xy}\sqrt{\frac{a+\rho}{\pi}}\cos^{-1}\left(\frac{a}{a+\rho}\right). \tag{4.2}$$

2.3 Calculation for the SIFs due to applied load

According to the SIF definition [35], the expressions for K_{I} and K_{II} for the crack with length l can be obtained by

$$K_{\mathrm{I}} = \lim_{x\to l}\left[\sqrt{2\pi\,(x-l)}\sigma_{yy}\right] = \frac{2\mu}{\pi\,(\kappa+1)}\lim_{x\to l}\left[\sqrt{2\pi\,(x-l)}\int_0^l \frac{\rho^{\perp}(\xi)}{x-\xi}\mathrm{d}\xi\right], \tag{5.1}$$

$$K_{\mathrm{II}} = \lim_{x\to l}\left[\sqrt{2\pi\,(x-l)}\sigma_{xy}\right] = \frac{2\mu}{\pi\,(\kappa+1)}\lim_{x\to l}\left[\sqrt{2\pi\,(x-l)}\int_0^l \frac{\rho^{\vdash}(\xi)}{x-\xi}\mathrm{d}\xi\right] \tag{5.2}$$

where σ_{yy} and σ_{xy} are the stress components due to the external loading and crack.

Equation (5) can be normalized to the interval $[-1, 1]$ by writing $\xi = \frac{l}{2}(1+t)$, $x = \frac{l}{2}(1+s)$. Setting $\phi^{\perp}(\mathrm{t}) = \sqrt{1-\mathrm{t}^2}\rho^{\perp}(\mathrm{t})$ and $\phi^{\vdash}(\mathrm{t}) = \sqrt{1-\mathrm{t}^2}\rho^{\vdash}(\mathrm{t})$, Eq. (5) is converted to the non-dimensional equations:

$$K_{\mathrm{I}} = \frac{2\mu}{\pi\,(\kappa+1)}\lim_{s\to 1}\left[\sqrt{\pi l\,(s-1)}\int_{-1}^{1}\frac{\phi^{\perp}(t))}{(s-t)\sqrt{1-t^2}}\mathrm{d}t\right], \tag{6.1}$$

$$K_{\mathrm{II}} = \frac{2\mu}{\pi\,(\kappa+1)}\lim_{s\to 1}\left[\sqrt{\pi l\,(s-1)}\int_{-1}^{1}\frac{\phi^{\vdash}(t)}{(s-t)\sqrt{1-t^2}}\mathrm{d}t\right]. \tag{6.2}$$

Thus,

$$K_{\mathrm{I}}^{\mathrm{L}} = \frac{\mu\sqrt{2\pi l}}{(\kappa+1)}\phi^{\perp}(1), \tag{7.1}$$

$$K_{\mathrm{I}}^{\mathrm{R}} = -\frac{\mu\sqrt{2\pi l}}{(\kappa+1)}\phi^{\perp}(-1), \tag{7.2}$$

$$K_{\mathrm{II}}^{\mathrm{L}} = \frac{\mu\sqrt{2\pi l}}{(\kappa+1)}\phi^{\vdash}(1), \tag{7.3}$$

$$K_{\mathrm{II}}^{\mathrm{R}} = -\frac{\mu\sqrt{2\pi l}}{(\kappa+1)}\phi^{\vdash}(-1) \tag{7.4}$$

where the superscripts L and R represent the left and right crack tips, respectively.

When the unknown dislocation densities $\rho^{\perp}$ and $\rho^{\vdash}$ are determined by an iteration procedure, the functions $\phi^{\perp}(t)$ and $\phi^{\vdash}(t)$ can be expressed as a polynomial of order N with unknown coefficients:

$$\phi(t) = \sum_{n=0}^{N} a_n t^n. \tag{8}$$

Using the least squares method the numerical solutions $\phi^{\perp}$ and $\phi^{\vdash}$, Eq. (7) can be written as

$$K_{\mathrm{I}}^{\mathrm{L}} = \frac{\mu\sqrt{2\pi l}}{(\kappa+1)}\sum_{n=0}^{N} a_n^{\perp}, \tag{9.1}$$

$$K_{\mathrm{I}}^{\mathrm{R}} = -\frac{\mu\sqrt{2\pi l}}{(\kappa+1)}\sum_{n=0}^{N}(-1)^n a_n^{\perp}, \tag{9.2}$$

$$K_{\mathrm{II}}^{\mathrm{L}} = \frac{\mu\sqrt{2\pi l}}{(\kappa+1)}\sum_{n=0}^{N} a_n^{\vdash}, \tag{9.3}$$

$$K_{\mathrm{II}}^{\mathrm{R}} = -\frac{\mu\sqrt{2\pi l}}{(\kappa+1)}\sum_{n=0}^{N}(-1)^n a_n^{\vdash}. \tag{9.4}$$

2.4 Numerical procedure for the entire problem

In order to solve for the plastic zones of the cracks, we assume the initial values, external load, and material parameters. Then, an iteration procedure is used to obtain the plastic zone sizes until the condition Eq. (2) is satisfied. More specifically, the stress distribution due to the cracks and inhomogeneous inclusions need first to be obtained. Then, the results for K_{I}, K_{II}, $K_{\mathrm{I}\rho}$, and $K_{\mathrm{II}\rho}$ can be calculated according to Eqs. (2.2) and (9). If $K_{\mathrm{I}} < K_{\mathrm{I}\rho}$, then ρ decreases. When $K_{\mathrm{I}} > K_{\mathrm{I}\rho}$, then ρ increases. If $K_{\mathrm{II}} < K_{\mathrm{II}\rho}$, then ρ decreases. When $K_{\mathrm{II}} > K_{\mathrm{II}\rho}$, then ρ increases. The procedure is repeated until the errors (between K_{I} and $K_{\mathrm{I}\rho}$, K_{II} and $K_{\mathrm{II}\rho}$) are small enough. The whole flowchart for the plastic zones of materials with multiple cracks and inhomogeneous inclusions in an isotropic infinite space subjected to the remote loading is shown in Fig. 4.

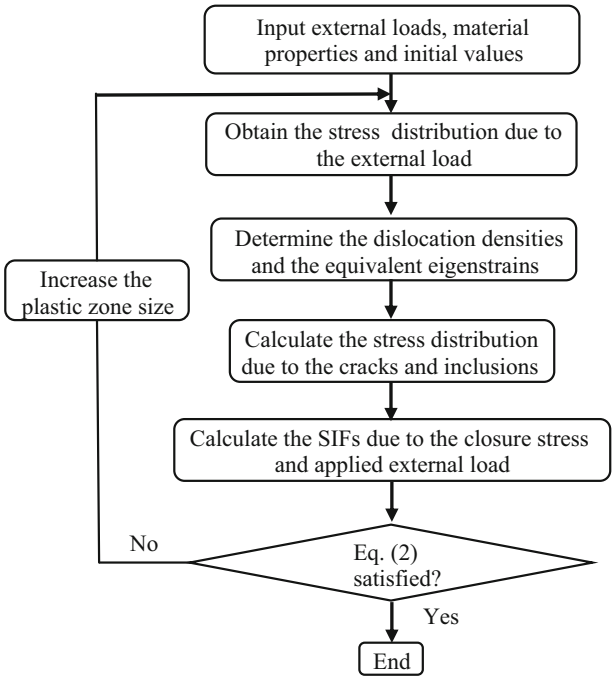

Fig. 4 Flowchart for the plastic zone sizes of the cracks interacting with inhomogeneous inclusions in an isotropic infinite space subjected to remote loading

3 Results and discussion

3.1 The model validation

In order to verify the proposed method to obtain the plastic zone sizes of cracks, the solution for a crack with original length $2a$ (a is a fixed value) beneath an infinite space under uniform tension T is considered. Its result is compared with the analytical solution of Dugdale. Figure 5 plots the effect of applied stress T over the yield stress of matrix materials ($\sigma_{\mathrm{YS}} = 600$ MPa) on the plastic zone size of crack tips in an infinite space under the remote tension stress. The results of the current method show a good agreement with the Dugdale analytical solution.

3.2 Plastic zones of two cracks in an infinite space

This part concerns the plastic zones of two cracks in an infinite space (Fig. 6) under the remote stress $\sigma_{yy}^{\infty} = 360$ MPa. The matrix is assumed to be steel ($E_S = 200$ GPa, $\sigma_{\mathrm{YS}} = 600$ MPa and $\upsilon_S = 0.28$); thus, the plastic

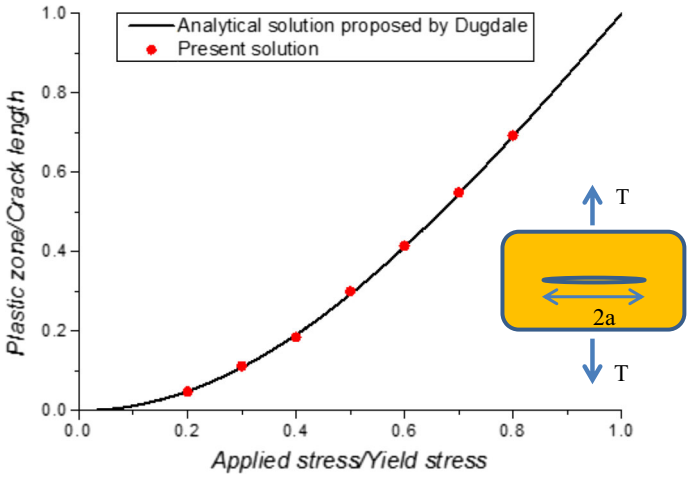

Fig. 5 Comparison of the Dugdale results with the present model

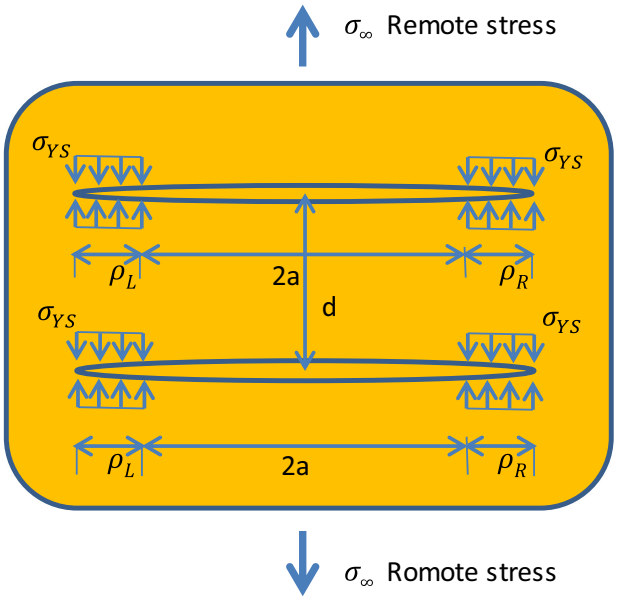

Fig. 6 Schematic of the plastic zones of two cracks in an infinite space under remote stress

zones will be governed by small-scale yielding. The original length of the two cracks is $2a$. The depth between these two cracks is set to be $d = \lambda a$. According to Fig. 7, the SIFs at the crack tips decrease clearly with the increment of the ratio $(2a/d)$, and a good agreement with the theoretical results and the current method can be found. Therefore, an accurate prediction for the plastic zone sizes of two cracks in an infinite space by the current model can be obtained.

Using the same material with the verified model, the plastic zone sizes and stress distribution of an infinite space with two cracks under the remote stress $\sigma_{yy}^{\infty} = 240$ MPa are studied. In this case, the depth between two cracks is fixed at $2.5a$, which means that the $2a/d$ is equal to 0.8. The computational domain $5a \times 4a$ is meshed in 100×80 elements. The contours of von Mises stress and the distribution of other stress components in the infinite space are presented in Fig. 8. The closure stresses applied on the plastic zones can be seen clearly. The plastic zone size ahead of the crack tips in this case is $0.4a$.

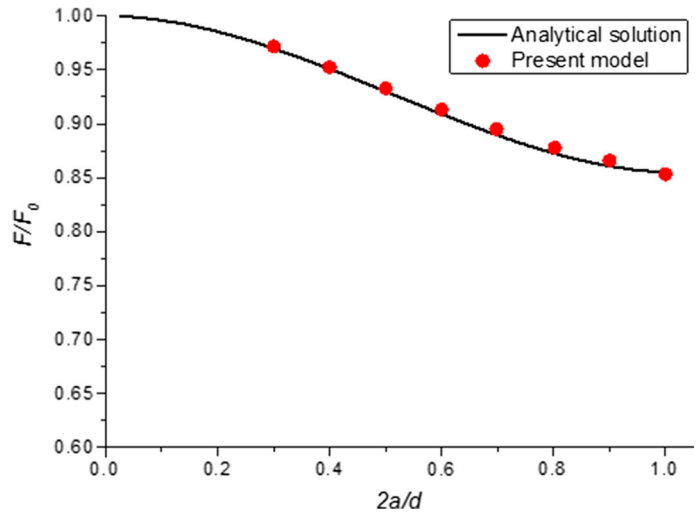

Fig. 7 SIFs of the model with two cracks in an infinite space under remote stress [36]

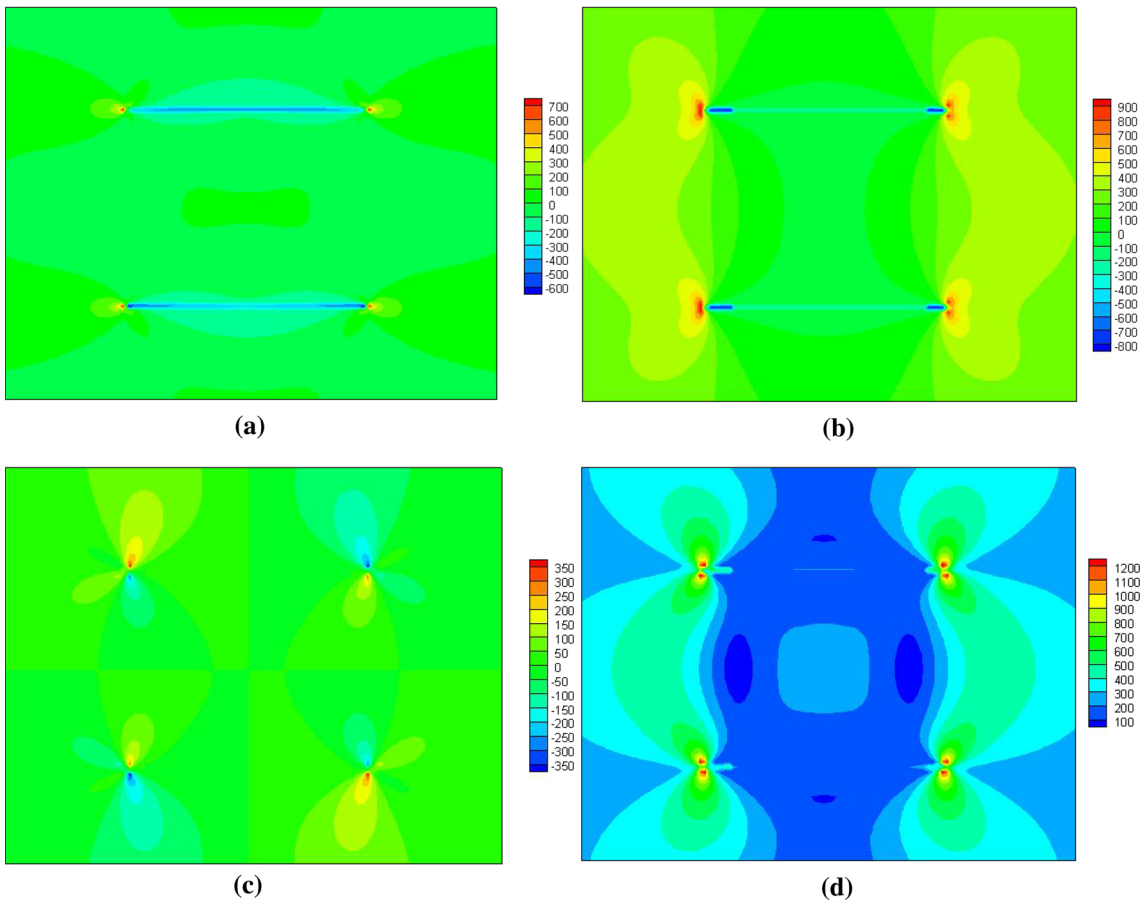

Fig. 8 The von Mises stress and other stress components distribution of two cracks in an infinite space: **a** σ_{xx}, **b** σ_{yy}, **c** τ_{xy}, and **d** σ_{VM}

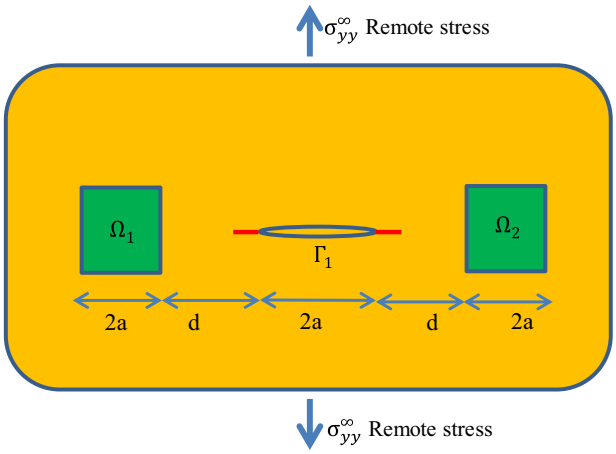

Fig. 9 Schematic of an isotropic infinite space with one crack interacting with two square inclusions ahead of crack tips under the remote stress

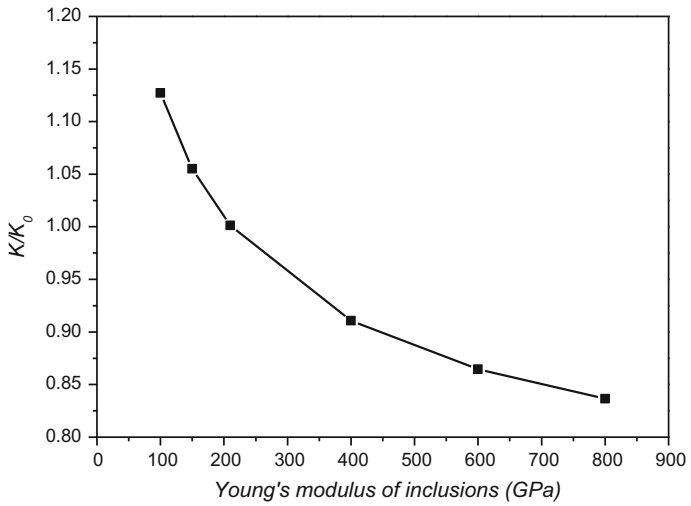

Fig. 10 SIFs of crack tips influenced by Young's modulus of inhomogeneous inclusions ahead of crack tips

3.3 One crack and two square inclusions ahead of crack tips

Figure 9 plots the schematic of an infinite space with two square inclusions ahead of one crack under the remote tension loading $\sigma_{yy}^{\infty} = 240$ MPa. The original length of the crack and side length of the inclusions are $2a$. The crack Γ_1 is centered at $(4a, 1.5a)$, and two inclusions Ω_1 and Ω_2 are centered at $(1.5a, 1.5a)$ and $(6.5a, 1.5a)$, respectively. The matrix has Young's modulus $E_S = 210$ GPa, Poisson's ratio $\upsilon_S = 0.28$, and yield stress $\sigma_{\mathrm{YS}} = 600$ MPa. The two inhomogeneous inclusions have the same Young's modulus $E_I = 400$ GPa and Poisson's ratio $\upsilon_I = 0.3$. The computational domain $8a \times 3a$ is discretized into 320×120 elements.

When the plastic zones of crack tips are not taken into account, it can be found from Fig. 10 that the SIFs of crack tips decrease gradually with the increment of Young's modulus of inhomogeneous inclusions. Here, K_0 is the SIF of the crack when no inclusions exist in the infinite space. It can be obtained when Young's modulus of inclusions satisfies the condition $E_S = E_I$. Afterward, the effect of Young's modulus of inclusions on the stress distribution and plastic zones of the crack in an infinite space is investigated. The detailed stress distribution for the case in which Young's modulus of the inclusions equals 400 GPa is plotted in Fig. 11. Moreover, as Young's modulus of the inclusions increases from 100 to 800 GPa, the ratio between the plastic zone size and the original half crack length decreases from to 0.4 to 0.175 as shown in Fig. 12.

Moreover, the effect of the distance d between the crack tip and inclusion side on the plastic zone size is also investigated. The results show that with the increment of d from $0.5a$ to $1.25a$ the ratio between the

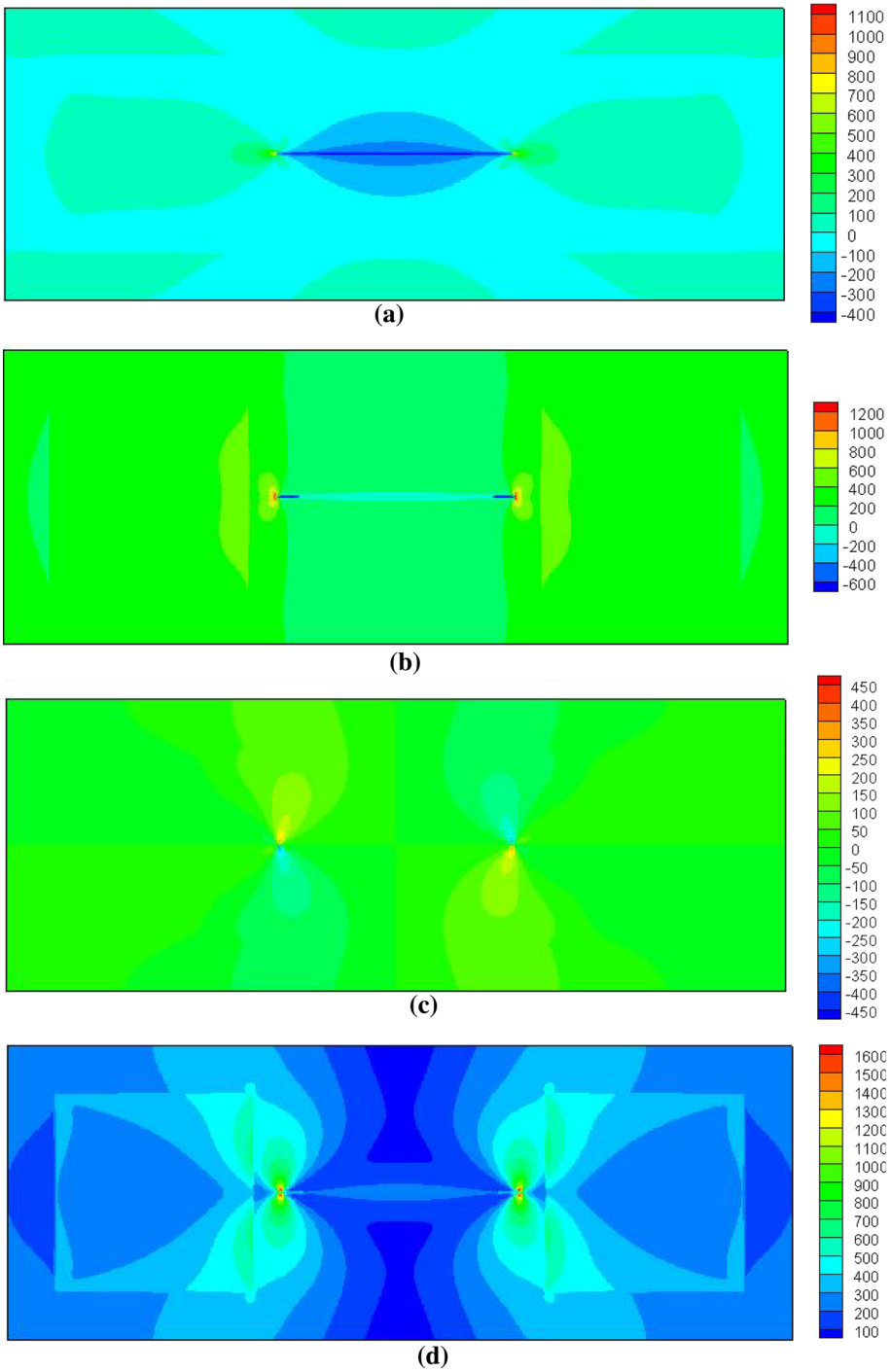

Fig. 11 The contours of stress components and von Mises stress distribution: **a** σ_{xx}, **b** σ_{yy}, **c** τ_{xy} and **d** σ_{VM}

plastic zone size at the crack tips and the original half crack length decreases from 0.4 to 0.275 according to Fig. 13. The effect of inhomogeneous inclusions on the plastic zone size of crack tips decreases dramatically with the increase of the distance d from $0.5a$ to $0.75a$, and this effect disappears when the distance d is larger than $1.25a$.

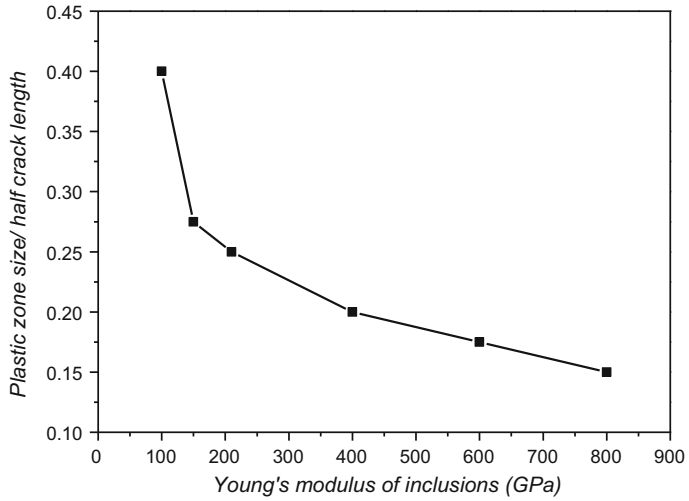

Fig. 12 The plastic zone size of one crack interacting with two inclusions ahead of crack tips with various Young's moduli

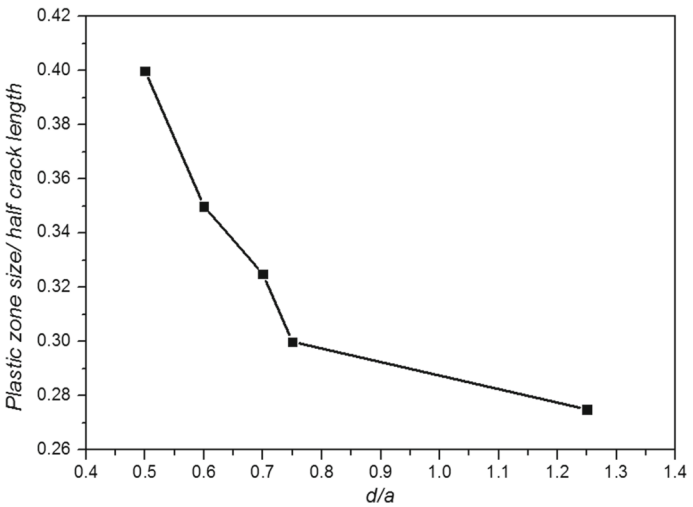

Fig. 13 The plastic zone size of one crack interacting with two inclusions ahead of crack tips with various distance between the crack tip and inclusions

3.4 Two square inclusions on both sides of one crack

Figure 14 illustrates two inhomogeneous inclusions on both sides of one crack in an infinite space subjected to the remote tension loading $\sigma_{yy}^{\infty} = 240$ MPa. The original length of the crack and side length of the inclusions are $2a$. The crack Γ_1 is centered at $(1.5a, 2.5a)$, and two inclusions Ω_1 and Ω_2 are centered at $(1.5a, 1.25a)$ and $(1.5a, 3.75a)$, respectively. The material parameters of matrix and inclusions in this part are the same as in Sect. 3.3. The computational domain $3a \times 5a$ is discretized into 120×200 elements.

When the plastic zones of crack tips are not taken into consideration, the trend of SIFs at the crack tips in this case is similar to that shown in Fig. 10. However, it can be seen from Fig. 15 that the influence of the inhomogeneous inclusions in this part is more significant than that in Part 3.3. Moreover, Fig. 16 shows the contours of the von Mises stress and other stress components in an infinite space with two square inhomogeneous inclusions ($E_I = 800$ GPa) on both sides of one crack; in this case the stress concentrations can be seen more clearly. It is found that the stresses at the corners around the inclusions in this case show weaker concentrations than in the above case. Figure 17 shows that the ratio between the plastic zone size and

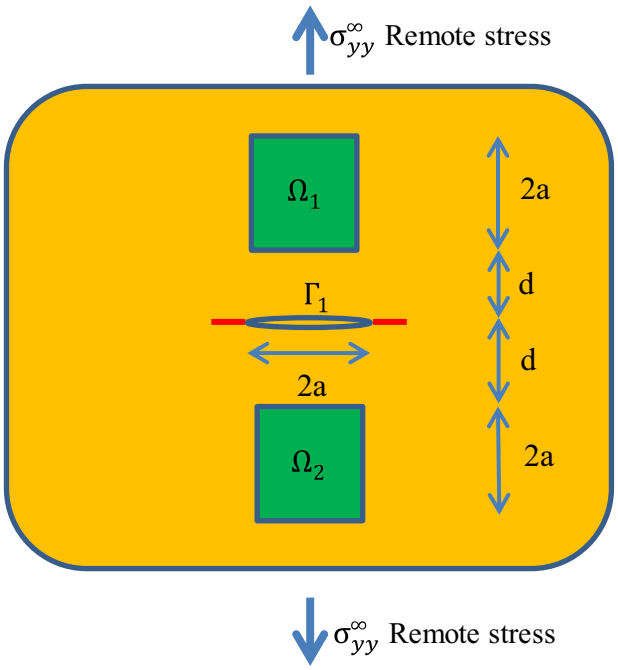

Fig. 14 Schematic of an isotropic infinite space with two inhomogeneous inclusions on both sides of one crack subjected to the remote tension stress

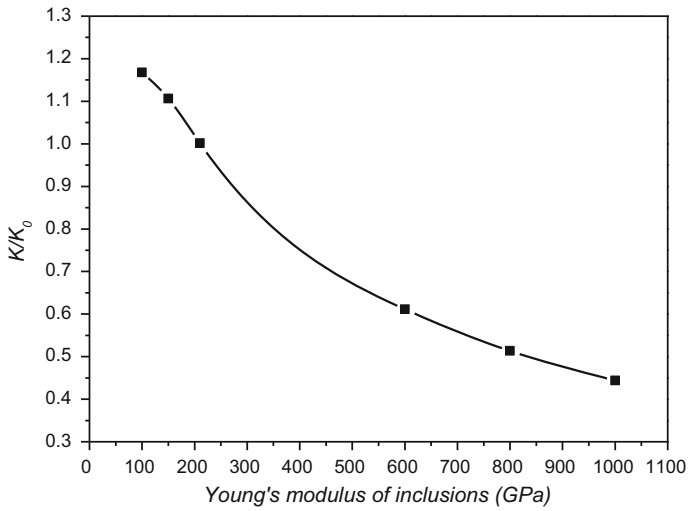

Fig. 15 SIFs of crack tips influenced by Young's modulus of inhomogeneous inclusions on both sides of one horizontal crack

original half crack length increases with the increment of Young's modulus of the inclusions on both sides of the crack. Moreover, it is also found that the effect of the distance between the crack and inclusions on the plastic zone size in this case is not very clear.

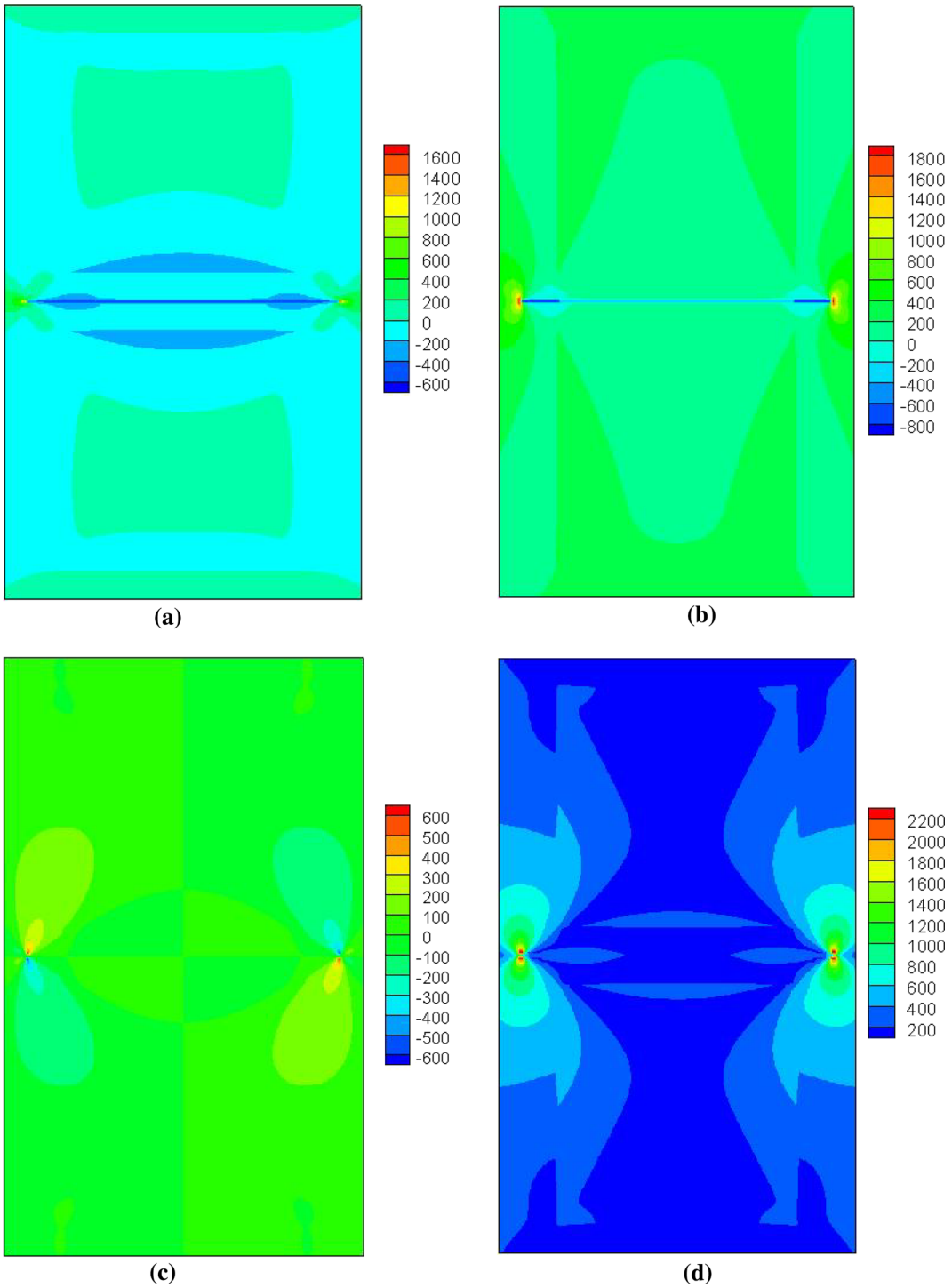

Fig. 16 The contours of stress components and von Mises stress distribution: **a** σ_{xx}, **b** σ_{yy}, **c** τ_{xy}, and **d** σ_{VM}

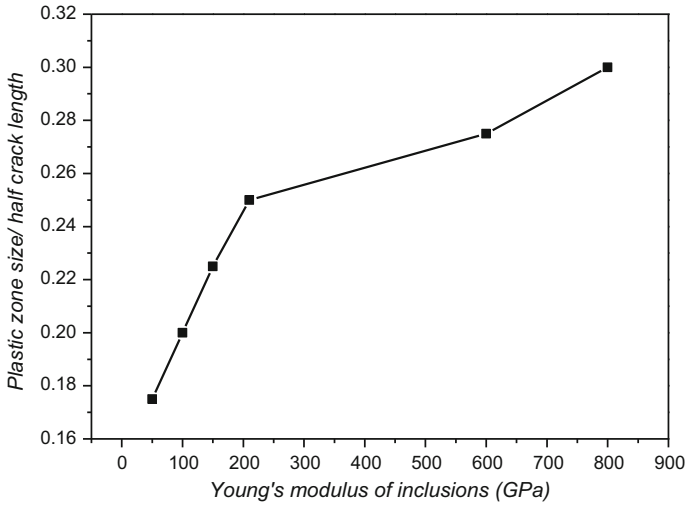

Fig. 17 The plastic zone size of one crack influenced by two inclusions on both sides with various Young's moduli

3.5 Two cracks and two square inclusions

Figure 18 shows the schematic of an infinite space with two inhomogeneous inclusions and two cracks subjected to the remote tension loading $\sigma_{yy}^{\infty} = 240$ MPa. The original length of the cracks and the side lengths of the inclusions are $2a$. Two cracks Γ_1 and Γ_2 are centered at $(4a, 0.5a)$ and $(4a, 2.5a)$, respectively. Two inclusions Ω_1 and Ω_2 are centered at $(1.5a, 1.5a)$ and $(6.5a, 1.5a)$, respectively. The material parameters of the matrix and inclusions in this Section are the same as in Sect. 3.3. The computational domain $8a \times 3a$ is discretized into 320×120 elements.

Figure 19 plots the contours of the stress components and von Mises stress for the case in which all the inclusions have the same Young's moduli $E_I = 600$ GPa. The plastic zone size of the crack tips in this case is $0.1a$. It can be found according to Fig. 20 that the ratio of the plastic zone size over the half crack length decreases from 0.275 to 0.1 with the increment of Young's inhomogeneous inclusions from 75 to 600 GPa.

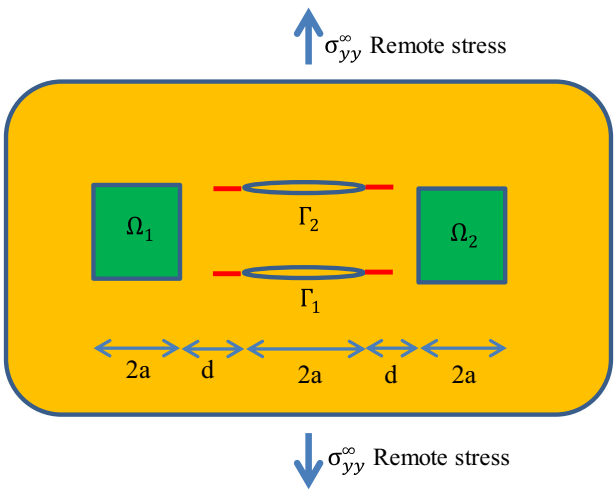

Fig. 18 Schematic of an isotropic infinite space with two cracks and two inhomogeneous inclusions subjected to the remote tension stress

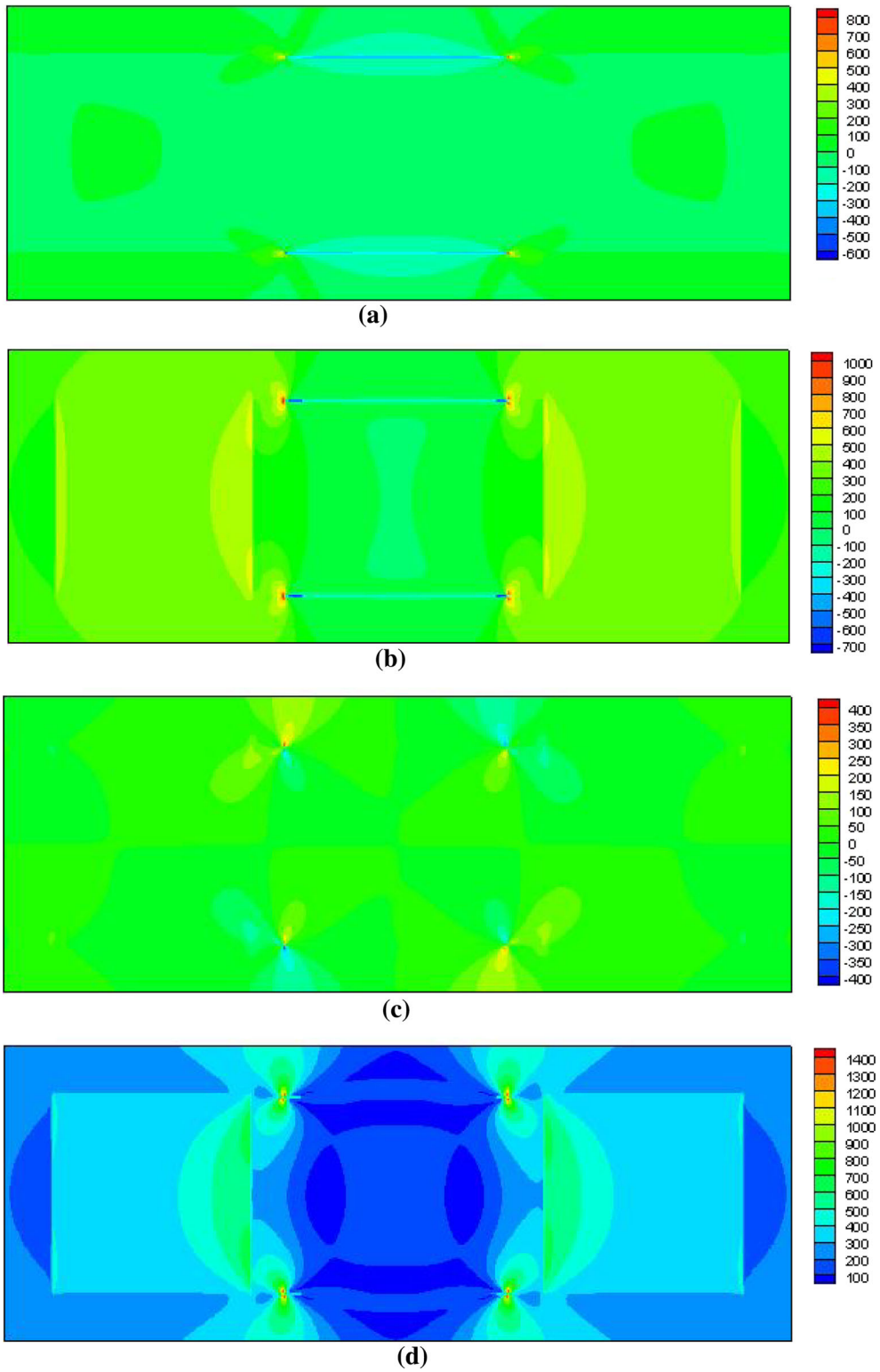

Fig. 19 The contours of stress components and von Mises stress distribution: **a** σ_{xx}, **b** σ_{yy}, **c** τ_{xy}, and **d** σ_{VM}

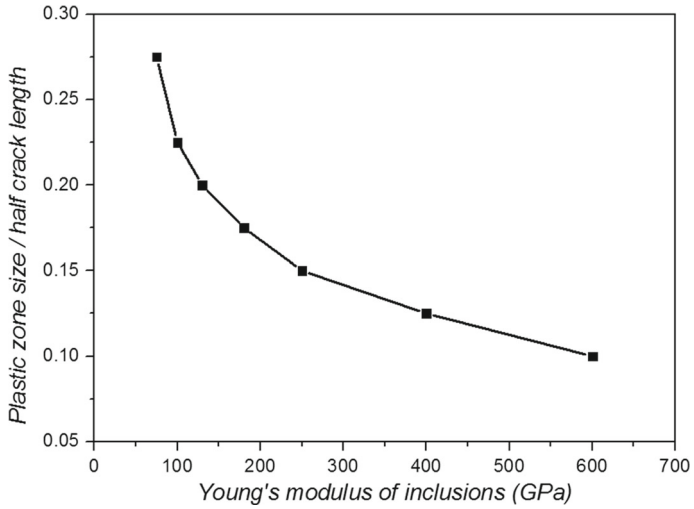

Fig. 20 The plastic zone size of crack tips influenced by two inclusions with various Young's moduli

4 Conclusions

This study provides a semi-analytical approach to study the plastic zones of an isotropic infinite space with multiple cracks interacting with inhomogeneous inclusions under the remote loading. To obtain this solution, a combined method with the EIM and DDT is applied. Using the DDT, each crack can be modeled by distributions of climb and glide dislocations with unknown densities to be determined. Each inhomogeneous inclusion can be treated as a homogeneous inclusion with initial eigenstrain plus the unknown equivalent eigenstrain based on the EIM. The advantage of this method is that it can treat multiple cracks and inclusions as it treats a single crack and inclusion without adding computational difficulties since all the cracks and inclusions are decomposed into many crack segments or rectangular inclusions at the beginning. The unknown dislocation densities and equivalent eigenstrains can be obtained by a conjugate gradient method. With the Dugdale model of small-scale yielding, plastic zones ahead of the crack tips are introduced whose size can be determined by canceling the SIF due to the closure stress and that due to the external applied load. The current model has been validated by comparison with the theoretical results of Dugdale. A group of simulations has been conducted to investigate the effect of Young's modulus and position of the inclusions on the plastic zone size of crack tips.

This solution has the ability to predict the plastic zones of an infinite space with multiple cracks interacting with inhomogeneous inclusions. Based on the works done by Zhou et al. [6,7], the present solution can be extended to solve the half-space problem with the consideration of the plastic zones of cracks.

Acknowledgements The authors acknowledge financial support by Singapore Maritime Institute (Grant No: SMI-2014-MA11) and the National Natural Science Foundation of China (Grant No: 11472200).

Appendix

When stresses within the equivalent inclusions are considered, the governing equation can be written according to Hooke's law and stress superposition:

$$C^{\psi}_{ijkl}C^{-1}_{klmq}(\sigma^{\mathrm{P}}_{mq}+\sigma^{*}_{mq}+\sigma^{\mathrm{c}}_{mq}+\sigma^{0}_{mq})-\sigma^{\mathrm{P}}_{ij}-\sigma^{*}_{ij}-\sigma^{\mathrm{c}}_{ij}-\sigma^{0}_{ij}+C^{\psi}_{ijkl}\varepsilon^{*}_{kl}=0$$
$$(\psi=1,2,...,w_{\mathrm{i}};\, i,j,k,l,m,q=1,2) \text{ within } \Omega_{\psi} \tag{A.1.1}$$

where σ^{P}_{ij} and σ^{*}_{ij} are the eigenstresses induced by all the initial eigenstrains $\varepsilon^{\mathrm{P}}_{ij}$ and all the equivalent eigenstrains ε^{*}_{ij}, respectively; σ^{c}_{ij} and σ^{0}_{ij} are the stresses caused by all the cracks and remote loading, respectively. The governing equation for each crack can be established:

$$\sigma^{\mathrm{P}}_{ij}+\sigma^{*}_{ij}+\sigma^{\mathrm{C}}_{ij}+\sigma^{0}_{ij}=0\,(i,\,j=1,2)\ \text{along}\ \Gamma_{\varphi} \tag{A.1.2}$$

where $i = 1$ for a crack perpendicular to the x-axis and $i = 2$ for a crack perpendicular to the y-axis.

According to the discretization method in the computational domain, the governing equation is given by

$$\begin{aligned}
&\left(\mathbf{C}_{\alpha,\beta}\mathbf{C}^{-1} - \mathbf{I}\right)\left[\sum_{\zeta=0}^{N_y-1}\sum_{\xi=0}^{N_x-1}\left(\mathbf{B}_{a-\xi,\beta-\zeta}\varepsilon^{*}_{\xi,\zeta} + \mathbf{B}_{a-\xi,\beta-\zeta}\varepsilon^{\mathrm{P}}_{\xi,\zeta}\right)\right.\\
&\left.+\frac{2\mu}{\pi\,(\kappa+1)}\sum_{\zeta=0}^{N_y-1}\sum_{\xi=0}^{N_x-1}\left(\mathbf{E}^{\perp}_{a-\xi,\beta-\zeta}c^{\perp}_{\xi,\zeta} + \mathbf{F}^{\perp}_{a-\xi,\beta-\zeta}d^{\perp}_{\xi,\zeta} + \mathbf{E}^{\vdash}_{a-\xi,\beta-\zeta}c^{\vdash}_{\xi,\zeta} + \mathbf{F}^{\vdash}_{a-\xi,\beta-\zeta}d^{\vdash}_{\xi,\zeta}\right)\right]\\
&+\mathbf{C}_{\alpha,\beta}\varepsilon^{*}_{\alpha,\beta} = 0 \quad \left(0 \le \alpha \le N_x - 1, 0 \le \beta \le N_y - 1\right) \text{ within } \Omega_{\psi}, \qquad \text{(A.2.1)}\\
&\sum_{\zeta=0}^{N_y-1}\sum_{\xi=0}^{N_x-1}\left(\mathbf{B}_{a-\xi,\beta-\zeta}\varepsilon^{\mathrm{P}}_{\xi,\zeta} + \mathbf{B}_{a-\xi,\beta-\zeta}\varepsilon^{*}_{\xi,\zeta}\right)\\
&+\frac{2\mu}{\pi\,(\kappa+1)}\sum_{\zeta=0}^{N_y-1}\sum_{\xi=0}^{N_x-1}\left(\mathbf{E}^{\perp}_{a-\xi,\beta-\zeta}c^{\perp}_{\xi,\zeta} + \mathbf{F}^{\perp}_{a-\xi,\beta-\zeta}d^{\perp}_{\xi,\zeta} + \mathbf{E}^{\vdash}_{a-\xi,\beta-\zeta}c^{\vdash}_{\xi,\zeta} + \mathbf{F}^{\vdash}_{a-\xi,\beta-\zeta}d^{\vdash}_{\xi,\zeta}\right) = 0\\
&\left(0 \le \alpha \le N_x - 1, 0 \le \beta \le N_y - 1\right) \text{ along } \Gamma_{\varphi}. \qquad \text{(A.2.2)}
\end{aligned}$$

where the coefficients $\mathbf{B}_{a-\xi,\beta-\zeta}$ relate the eigenstresses $\boldsymbol{\sigma}^{\mathrm{P}}_{\alpha,\beta}$ and $\boldsymbol{\sigma}^{*}_{\alpha,\beta}$ at the observation point (x_α, y_β) in the square element $[\alpha, \beta]$ to the initial eigenstrain $\boldsymbol{\varepsilon}^{\mathrm{P}}_{\xi,\zeta}$ and equivalent eigenstrain $\boldsymbol{\varepsilon}^{*}_{\xi,\zeta}$ in the element $[\xi, \zeta]$, respectively; $\mathbf{E}^{\perp}_{a-\xi,\beta-\zeta}$, $\mathbf{F}^{\perp}_{a-\xi,\beta-\zeta}$, $\mathbf{E}^{\vdash}_{a-\xi,\beta-\zeta}$ and $\mathbf{F}^{\vdash}_{a-\xi,\beta-\zeta}$ are the influence coefficients relating the stresses to the dislocation density parameters. The unknowns can be obtained by solving the governing equation using the conjugate gradient method. The fast Fourier transform algorithm is applied to improve the computational efficiency.

Acknowledgements The authors acknowledge financial support by Singapore Maritime Institute (Grant No: SMI-2014-MA11) and the National Natural Science Foundation of China (Grant No: 11472200).

References

1. Kachanov, M.: Elastic solids with many cracks—a simple method of analysis. Int. J. Solids Struct. **23**(1), 23–43 (1987)
2. Xiao, Z.M., Yan, J., Chen, B.J.: Electro-elastic stress analysis for a Zener–Stroh crack interacting with a coated inclusion in a piezoelectric solid. Acta Mech. **171**(1–2), 29–40 (2004)
3. Fang, Q.H., Liu, Y.W.: Size-dependent interaction between an edge dislocation and a nanoscale inhomogeneity with interface effects. Acta Mater. **54**(16), 4213–20 (2006)
4. Fang, Q.H., Jin, B., Liu, Y., Liu, Y.W.: Interaction between screw dislocations and inclusions with imperfect interfaces in fiber-reinforced composites. Acta Mech. **203**(1–2), 113–25 (2009)
5. Li, Z., Li, Y., Sun, J., Feng, X.Q.: An approximate continuum theory for interaction between dislocation and inhomogeneity of any shape and properties. J. Appl. Phys. **109**(11), 113529 (2011)
6. Zhou, K., Wei, R.B.: Modeling cracks and inclusions near surfaces under contact loading. Int. J. Mech. Sci. **83**, 163–71 (2014)
7. Zhou, K., Wei, R.B.: Multiple cracks in a half-space under contact loading. Acta Mech. **225**(4–5), 1487–502 (2014)
8. Dong, Q.B., Zhou, K.: Multiple inhomogeneous inclusions and cracks in a half space under elastohydrodynamic lubrication contact. Int. J. Appl. Mech. **7**(1), 1550003 (2015)
9. Dong, Q.B., Zhou, K.: Elastohydrodynamic lubrication modeling for materials with multiple cracks. Acta Mech. **225**(12), 3395–408 (2014)
10. Wang, X., Zhou, K.: An inclusion of arbitrary shape in an infinite or semi-infinite isotropic multilayered plate. Int. J. Appl. Mech. **6**(1), 1450001 (2014)
11. Zhou, K.: Elastic field and effective moduli of periodic composites with arbitrary inhomogeneity distribution. Acta Mech. **223**(2), 293–308 (2012)
12. Zhou, K., Wei, R.B., Bi, G.J., Wang, X., Song, B., Feng, X.Q.: Semi-analytic solution of multiple inhomogeneous inclusions and cracks in an infinite space. Int. J. Comput. Methods **12**(1), 1550002 (2015)
13. Tao, Y.S., Fang, Q.H., Zeng, X., Liu, Y.W.: Influence of dislocation on interaction between a crack and a circular inhomogeneity. Int. J. Mech. Sci. **80**, 47–53 (2014)
14. Khan, S.M.A., Khraisheh, M.K.: Analysis of mixed mode crack initiation angles under various loading conditions. Eng. Fract. Mech. **67**(5), 397–419 (2000)
15. Khan, S.M.A., Khraisheh, M.K.: A new criterion for mixed mode fracture initiation based on the crack tip plastic core region. Int. J. Plast. **20**(1), 55–84 (2004)

16. Bian, L.C., Kim, K.S.: The minimum plastic zone radius criterion for crack initiation direction applied to surface cracks and through-cracks under mixed mode loading. Int. J. Fatigue **26**(11), 1169–78 (2004)
17. Golos, K., Wasiluk, B.: Role of plastic zone in crack growth direction criterion under mixed mode loading. Int. J. Fract. **102**(4), 341–53 (2000)
18. Achenbach, J.D., Keer, L.M., Khetan, R.P., Chen, S.H.: Loss of Adhesion at the Tip of an Interface Crack. J. Elast. **9**(4), 397–424 (1979)
19. Irwin, G.: Linear fracture mechanics, fracture transition, and fracture control. Eng. Fract. Mech. **1**(2), 241–57 (1968)
20. Dugdale, D.S.: Yielding of steel sheets containing slits. J. Mech. Phys. Solids **8**(2), 100–4 (1960)
21. Hoh, H.J., Xiao, Z.M., Luo, J.: On the plastic zone size and crack tip opening displacement of a Dugdale crack interacting with a circular inclusion. Acta Mech. **210**(3–4), 305–14 (2010)
22. Hoh, H.J., Xiao, Z.M., Luo, J.: On the plastic zone size and CTOD study for a Zener–Stroh crack interacting with a circular inclusion. Acta Mech. **220**(1–4), 155–65 (2011)
23. Yi, D.K., Xiao, Z.M., Zhuang, J., Sridhar, I.: On the plastic zone size and crack tip opening displacement of a sub-interface crack in an infinite bi-material plate. Philos. Mag. **91**(26), 3456–72 (2011)
24. Yi, D.K., Xiao, Z.M., Tan, S.K.: On the plastic zone size and the crack tip opening displacement of an interface crack between two dissimilar materials. Int. J. Fract. **176**(1), 97–104 (2012)
25. Hoh, H.J., Xiao, Z.M., Luo, J.: Plastic zone size and crack tip opening displacement of a Dugdale crack interacting with a coated circular inclusion. Philos. Mag. **90**(26), 3511–30 (2010)
26. Fan, M., Xiao, Z.M., Luo, J.: On the plastic zone correction of a Zener–Stroh crack interacting with a nearby inhomogeneity and an edge dislocation. Acta Mech. **226**(12), 4173–88 (2015)
27. Fan, M., Yi, D., Xiao, Z.: An interfacial arc-shaped Zener–Stroh crack due to inclusion-matrix debonding in composites. Acta Mech. **225**(3), 909–18 (2014)
28. Fan, M., Yi, D.K., Xiao, Z.M.: Elastic–Plastic fracture behavior analysis on a Griffith crack in the cylindrical three-phase composites with generalized Irwin model. Int. J. Appl. Mech. **6**(4), 1450045 (2014)
29. Fan, M., Yi, D.K., Xiao, Z.M.: Elastic–plastic stress investigation for an arc-shaped interface crack in composite material. Int. J. Mech. Sci. **83**, 104–11 (2014)
30. Fan, M., Yi, D.K., Xiao, Z.M.: A Zener–Stroh crack in fiber-reinforced composites with generalized Irwin plastic zone correction. Int. J. Mech. Sci. **82**, 81–9 (2014)
31. Fan, M., Yi, D.K., Xiao, Z.M.: Generalized Irwin plastic zone correction for a Griffith crack near a coated-circular inclusion. Int. J. Damage Mech. **24**(5), 663–82 (2015)
32. Fan, M., Yi, D.K., Xiao, Z.M.: Fracture behavior investigation on an arbitrarily oriented sub-interface Zener–Stroh crack. Acta Mech. **226**(5), 1591–603 (2015)
33. Jing, P.H., Khraishi, T., Gorbatikh, L.: Closed-form solutions for the mode II crack tip plastic zone shape. Int. J. Fract. **122**(3–4), L137–L42 (2003)
34. Feng, X.Q., Li, H.Y., Yu, S.W.: A simple method for calculating interaction of numerous microcracks and its applications. Int. J. Solids Struct. **40**(2), 447–64 (2003)
35. Anderson, T.L., Anderson, T.: Fracture Mechanics: Fundamentals and Applications. CRC Press, Boca Raton (2005)
36. Murakami, Y.: Stress Intensity Factors Handbook, 1st edn. Pergamon, Oxford (1987)